A Data Exchange Algorithm for One Way Fluid-Structure Interaction Analysis and its Application on High-Speed Train Coupling Interface

S. Huang, Y. Xu, L. Zhang† and W. Zhu

School of Mechanical, Electronic and Control Engineering, Beijing, 100044, China

†*Corresponding Author Email: llzhang1@bjtu.edu.cn*

ABSTRACT

Domain decomposition is involved in Fluid-Structure Interaction (FSI) analysis to speed up their computations. Non-matched meshes always exist in the interface of these different domains which brings data exchange problem. A load transfer method is investigated in this article to deal with non-matching meshes between fluid and structure. The local nearest neighbor searching algorithm was used in this method to match fluid nodes and structural elements, while thin plate splines with tension were used to deal with data transfer between non-matching meshes in FSI computations, and the corresponding matrix equations for the target points are presented. Implementations of the obtained algorithms were used to solve the one-way FSI problem of the CRH380C high-speed train and the relative error of transferred results was analyzed. The statistical parameters under two algorithms, the TPS model and the model combining both TPS model and nearest interpolation model were compared and the results indicate that the latter can transfer data more accurately.

Keywords: Load transfer method; High-speed train; Data exchange; Interpolation method; Thin plate spline with tension.

NOMENCLATURE

A_{ff}	coefficient matrix of fluid domain	$K_0(d\varphi)$	modified zeroth order Bessel function
A_{ss}, B_s, ΔX_s^k	parameters of solid domain	P_{s0}	unknown pressure in Node 0
A_{fs}, A_{sf}	coupling matrix	R_d	basis function
B_f	external forces of fluid domain	V_c	train velocity vector
c	constant 0.577215		
d_{ij}	euclidean length		
$D(\xi_{e^r})$	population variance of the relative error	α	trend function
		ϕ	flow flux
e^r_{p*}	relative error of pressure load	φ	weight value
$E(\xi_{e^r})$	expected value of relative error	ΔX_f^k	unknown forces of the fluid domain
F_a	aerodynamic torque	$\frac{n(e^r_{p*})}{N}$	percentage rates of relative error
$H(\phi)$	integral function		
k	iterative time step		

1. INTRODUCTION

One-way Fluid-Structure Interaction analysis is commonly used to deal with FSI problems in high-speed trains. According to this methodology, CFD (Computational Fluid Dynamics) and CSD (Computational Solid Dynamics) solvers should couple on the solid-fluid interfaces where the structural nodal position, displacement and loads are exchanged between the two solvers. The loading data and boundary conditions can be exchanged

accurately when the two solvers are using a uniform mesh. However, different meshes are usually used in the two domains based on different discretization scheme of the above two solvers. After several decades of research, many coupling interpolation methods have been proposed to deal with FSI problems; these methods can be divided into partitioned interpolation methods and integral interpolation methods. When using the partitioned interpolation method to carry out fluid-solid coupling data transfer, partial node or element data are introduced to calculate the corresponding

unknown node or element information. Some commonly partitioned interpolation methods are the projection method (Boer, Zuijlen, and Bijl 2007), Constant Volume Transformation (CVT) (Goura, Badcock, Woodgate, and Richards 2001), etc. When using the integral interpolation methods, on the contrary, all node and element information is required. The splines' interpolation method (Harder and Desmarais 1972), Inverse Isoparametric Mapping (Pidaparti 1992) and the Shepard method (Shepard 1968) (SU, Qian, and Yuan 2010) are common examples of this family of methods.

When applying the projection method, the node displacement in the fluid domain is assumed to be equal to the displacement of the projection points in the solid domain, and can be obtained using shape function interpolation in that solid element. This method is easy to understand and apply, but its disadvantage is that the overall displacement coordination and force equivalence of the interface is not considered, which greatly limits its applications. Goura *et al*. (Goura, Badcock, Woodgate, and Richards 2001) first proposed a method called Constant Volume Transformation (CVT), which is a partitioned interpolation method where element volume conservation is central, and does not rely on information from the structural model. This method is based on the assumption that the orthogonal projection of the aerodynamic points in the structure triangle remains constant and is in accordance with the linear elastic properties of the solid surface element. For the calculation, as long as the volume of the tetrahedron, which is composed of the structure triangle and pneumatic points, is conserved, the length of the aerodynamic point beyond the plate can be calculated. The adaptability of this method, however, is not very good, as there are usually some anomalies which cannot be calculated, and its accuracy needs to be improved (Xu and Chen 2004). An improved CVT method that introduced area limits to ensure the quality of grid interpolation has been proposed by Min Xu and Shiqi Chen (Xu and Chen 2004). This improved CVT interpolation method avoids the abnormal cases of the original CVT method and greatly improves the interpolation precision. The improved CVT method, however, also requires the nodes mapping relationship, and the assumption of constant volume will also increase the complexity of calculations. The Shepard method (Shepard 1968), also known as the penultimate weighting method, was first used in meteorology and geological exploration. This method defines the value of an unknown point as the distance-reciprocal weighted sum of the values of the known points within a specific neighbourhood. Although the Shepard interpolation is smooth, the derivative values near the known point of the interpolation function are zero, which affects its accuracy. If the second or third derivative of the function at these points is known, this problem can be solved by constructing an improved Shepard interpolation or an interpolation with derivative conditions (SU, Qian, and Yuan 2010). In 1971, Harder first proposed the Infinite Plate Spline (IPS) (Harder and

Desmarais 1972), which is based on the superposition solution of differential equilibrium equations with regard to an infinite plate. Appa (Appa 1989), however, believed that it is not reliable to extrapolate the target value of the plate edge from the grid points inside the plate while using the IPS method. In this context, the Finite Surface Spline Method, the Thin-plate Spline Method, and the Multiquadric-Biharmonic Method have been put forwards. More details about these methods can be found in Smith's article (Smith, Hodges, and Cesnik 1995). In recent years, the mathematical community has conducted a lot of research on the approximate method based on Radial Basis Function (RBF). Interpolation methods based on the radial basis function can be used for processing large amounts of bulk random data and is widely used in computer graphics, meteorology, topography and other fields.

It is always possible to use off-the-shelf commercial software to analyze high-speed train FSI problems. However, although such software is easy to use and computationally efficient, it is difficult to control the relative error. Also, this interpolation algorithms with constant parameters that commercial software used do not fit well to the specific shape of high-speed train which contains lots of surfaces with different curvature. Therefore, we propose a new FSI algorithm to transfer the data from the CFD solver to CSD solver. This algorithm combines the nearest interpolation model with the Thin Plate Spline with Tension (TPS) model. The nearest neighbor interpolation model is always present in common commercial software and the TPS radial basis function is based on a vast scope of theoretical studies from Frank R. (Frank 1982) and Wu Z. M. (Wu 1995) *et al*. The proposed algorithm solves the problems mentioned above and performs the automatic link-up of the fluid and solid interface, it automatically identifies different mesh types, matches the fluidic nodes to the structural elements and achieves accurate coupling.

2. THE LOOSE FLUID-SOLID INTERAC- TION METHOD IN HIGH-SPEED TRAIN-S

2.1 Governing Equations

Combined with train dynamics equations and the fluid flow governing equations, the FSI governing equations (Zhang 2013) of high-speed trains have the form of Eq. (1), where v_c is the train velocity vector, F_a is the aerodynamic torque, and F_a can be expressed as the integral function H, which is related with flow flux ϕ .

$$
\begin{cases}
\dfrac{\partial}{\partial t}\int_V \rho\phi dv + \int_A n.(\rho(v-\bar{v})\phi)dA = \int_A n.(\Gamma grad\phi)dA + \int_V SdV \\
\bar{v} = v_c \\
F_a = H(\phi) \\
M\dot{\rho} + C_P^\lambda\lambda = Q_e + Q_v + Q_{wr} + F_a
\end{cases}
$$

$$(1)$$

These equations are the basic governing equations for dealing with FSI problems. In order to facilitate the analysis and solve the equations, the general form of the equations is established, different parameter values are given, and appropriate initial conditions and boundary conditions are defined. Currently, there are two approaches to the solution of FSI problems: either using directly coupled solution (Hermann, Matthies, Rainer, and Jan 2006) or partitioned solution, i.e. the loose method (Lohner, Yang, and Cebral 1998) (Keith, Richard, Vinay, and Tayfun 2000) (Tayfun, Sunil, Ryan, and Keith 2006) (Bell, Burton, Thompson, Herbst, and Sheridan 2014). Directly coupled solutions, or strong coupling, deal with the FSI problems by solving the combined equations directly. That is to say, the solid and fluid flow governing equations are solved using one solver. The coupled matrix is as follows:

$$
\begin{bmatrix} A_{ff} & A_{fs} \\ A_{sf} & A_{ss} \end{bmatrix} \begin{bmatrix} \Delta X_f^k \\ \Delta X_s^k \end{bmatrix} = \begin{bmatrix} B_f \\ B_s \end{bmatrix}
\tag{2}
$$

Here, k is iterative time step, A_{ff}, B_f and ΔX_f^k are the coefficient matrices, external forces and unknown forces of the fluid domain, respectively, A_{ss}, B_s and ΔX_s^k are the parameters of the solid domain, and A_{fs} and A_{sf} are the coupling matrices.

As there is no time delay after coupling solving, directly coupled solution is thought to be ideal solution. However, this solution can hardly combine the existing CFD and CSD techniques. Moreover, it converges slowly and cannot deal with large amounts of data. Directly coupled solution can at present be only applied to simple problems in FSI, and has not been used in complex engineering applications. Partitioned solution, in contrast, needs not solve the solid dynamics and the fluid flow governing equations simultaneously. This method solves the two equations separately, and, by transferring data between different solvers, can reach the final convergence result.

2.2 Analysis of the Loose Fluid-Solid Interaction Method

When we analyze FSI problems on high-speed train bodies, the influence of pressure on the train caused by outflow is much greater than the train's displacement deformation due to outflow. The difference is so large that one-way FSI is much more significant than two-way FSI. Therefore, this article focuses on one-way FSI analysis on a high-speed train body. The coupling parameters ①③⑤ presented in Fig. 1 transfer from fluid to solid as the computational time goes by. Unmatched meshes occur in the fluid-solid interface due to the application of different solvers. This process should also make sure data are exchanged accurately when unmatched meshes exist in the two domains. The nearest interpolation model, which is commonly used by commercial software, can deal with matched meshes or slightly unmatched meshes. However,

during the modelling process of actual engineering project, certain matched or slightly unmatched meshes are usually not happening the most of time because different grid discrete schemes are adopted in the fluid domain and the solid domain (Farhat, Lesionne, and LeTallec 1998) (Smith and Hodges 2000) (Boer, Zuijlen, and Bijl 2007). Instead, the most cases will be as Fig. 2 shows.
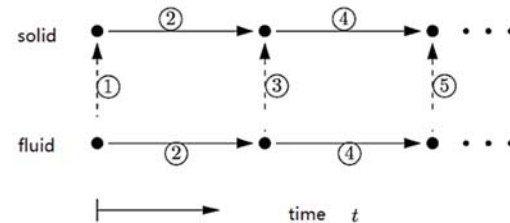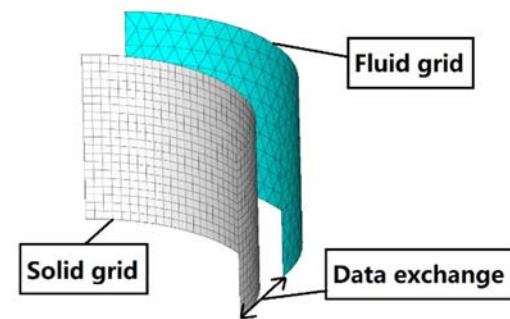

Fig. 1. Data transfer of one-way FSI.

Fig. 2. Non-matching meshes.

3. LOAD TRANSFER

3.1 Local nearest Searching

The high-speed train body is a type of large FSI interface where the loss of coupling details is not allowed. Local interpolation is more accurate than global interpolation, so, in order to use it, the local nearest searching method is adopted. That is, a local interpolation region is built centered on every data point that forms the receiving target and the nearest source data points are searched and the interpolation model is applied on this local region.

3.2 Thin Plate Spline with Tension Interpolation Model

The Thin Plate Spline with Tension (Benbourhim and Bouhamidi 2005) (Smith, Cesnik, and Hodges 1995) makes use of the Radial Basis Function (RBF) (Frank 1982) (Wu 1995) (Smith, Cesnik, and Hodges 1995) (Tiago and Leitão 2006). It is widely used in Geographic Information Systems' technology. The TPS provides a mean to characterize an irregular surface by using functions that minimize an energy function. In other words, the TPS can fit all source data using a minimum curvature surface. The TPS and its variations can be applied to smooth and continuous surfaces, and are also used in aeroelastic applications and high-speed vehicles.
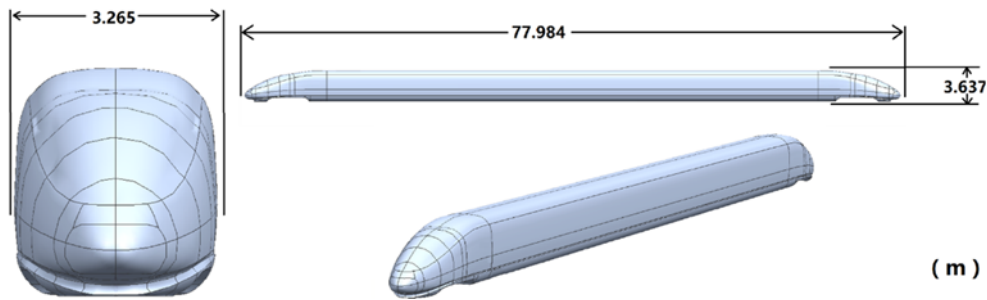
Fig. 3. Geometry model of 3-trainset high speed train CRH380C.

The Thin Plate Spline with Tension takes the form:

$$a + \sum_{i=1}^{n} A_i R_{d_i} \qquad (3)$$

where a is the trend function, and R_d is the basis function, whose full form is shown in Eq.(4).

$$R_d = -\frac{1}{2\pi\varphi^2}\left[\ln\frac{d\varphi}{2} + c + K_0(d\varphi)\right] \qquad (4)$$

Here, φ is the weight value, whose range is (0, 1). A high φ will reduce plate stiffness, hence it will lead final surface shape that is too flexible, like film (Frank 1982). After many simulations, φ was defined as 0.2. c is constant, with a value of 0.577215(Wu 1995), and $K_0(d\varphi)$ is a modified zeroth order Bessel function, which is formulated using Eqs. (5) and (6)

$$K_\nu(z) = \frac{\pi}{2}\frac{I_{-\nu}(z)}{\sin(\nu\pi)} \qquad (5)$$

$$I_\nu(z) = (\frac{z}{2})^\nu \sum_{k=0}^{\infty}\frac{(\frac{z^2}{4})^k}{k!\Gamma(\nu+k+1)} \qquad (6)$$

Based on the theory of Thin Plate Spline with Tension, the target's interpolation formulation can be derived as follows. After local nearest searching, in the 0 subdomain, for example, the unknown pressure P_{s0} of the solid node and nth known pressure $P_{l1}, P_{l2}, \cdots, P_{ln}$ in the fluid domain are on the same governing thin plate. We can get Eq. (7) when combining the constraint condition and Eqs.(3), (4), (5),(6). After solving for the unknown coefficients in Eq. (7), we can substitute them back into Eq. (3). Then, the final equation for P_{s0} is obtained (Eq. (8)), while the parameters $R_{d_{ij}}$ (i, j = 0, 1, 2,··· ,n) are determined using Eqs. (4), (5) and (6), where d_{ij} is the Euclidean length. Following this, we can calculate $[P_{s1}\ P_{s2}\ ...\ ...\ P_{sn}]^T$, as all we need to obtain is $[P_{l1}\ P_{l2}\ ...\ ...\ P_{ln}]^T$, which can be obtained through local nearest neighbor searching, as mentioned in subsection 3.1.

3.3 Nearest Interpolation Model

The main idea of nearest interpolation model (Thévenaz, Blu, and Unser 2000) is considerably different to the Radial Basis Function. A search algorithm determines the point x_A in mesh A that is closest to a given point x_B in mesh B. The value for the variable in x_B is set equal to that of x_A. In this manner, its coupling matrix is a $n_s \times n_f$ Boolean matrix. Every row has only one nonzero number that is equal to one. Moreover, the coefficient matrix is sparse, and all the nonzero elements in it are gather on the diagonal or near it. So, stable solutions of the linear equations can be obtained. Then, only a small summation is needed to solve after obtaining the solutions of the coefficients of the interpolation function. Therefore, this model is suitable for areas where the meshes match, and does not impose a significant computational load.

3.4 Load Transfer Process

The high-speed train CRH380C's geometric model was built using UG NX8, its outflow field meshes were formed using Ansys ICEM and its FE model was built using Hypermesh, all commercially available products. The flow field model of two passing trains is entered into Fluent to calculate the pressure. Then, these results for the train surface were output to MATLAB for TPS Analysis to build the interpolation problem after fluidic nodes and structural elements were matched using local nearest neighbor searching. In the subsequent step, the interpolation problem formed is submitted to our solver using the TPS model and nearest neighbor interpolation model to calculate the loading pressure on each structural element. The results obtained can then be directly input to Ansys or Abaqus for further mechanical analysis.

4. NUMERICAL APPLICATION IN HIGH- SPEED TRAIN AND RESULTS

Two passing trains in open air at high speed induces transient changes of aerodynamic pressure in its exterior environment. These intense pressure changes will affect the safety of train body and its components. One needs to know the aerodynamic load on structure if we want to know how exactly the affection is. By bringing oneway FSI technique, we can transfer those data to train body. Following the purposes, the models of two passing trains in open air conditions were created. The geometrical parameters of the 3-trainset CRH380C are shown in Fig. 3, along with the dimensions used for the aerodynamical domain's computations domain

$$\begin{bmatrix} 1 & 0 & R_{d12} & R_{d13} & ... & R_{d1n} \\ 1 & R_{d21} & 0 & R_{d23} & ... & R_{d2n} \\ \vdots & \vdots & \vdots & \ddots & & \vdots \\ \vdots & \vdots & \vdots & & \ddots & R_{d(n-1)n} \\ 1 & R_{dn1} & ... & ... & R_{dn(n-1)} & 0 \\ 0 & 1 & \vdots & \vdots & \vdots & 1 \end{bmatrix} \begin{bmatrix} a \\ A_1 \\ \vdots \\ \vdots \\ A_n \\ 0 \end{bmatrix} = \begin{bmatrix} P_{l1} \\ P_{l2} \\ \vdots \\ \vdots \\ P_{ln} \\ 0 \end{bmatrix}$$

$$(7)$$

$$P_{s0} = \begin{bmatrix} P_{l1} \\ P_{l2} \\ \vdots \\ \vdots \\ P_{ln} \\ 0 \end{bmatrix}^T \left(\begin{bmatrix} 1 & 0 & R_{d12} & R_{d13} & ... & R_{d1n} \\ 1 & R_{d21} & 0 & R_{d23} & ... & R_{d2n} \\ \vdots & \vdots & \vdots & \ddots & & \vdots \\ \vdots & \vdots & \vdots & & \ddots & R_{d(n-1)n} \\ 1 & R_{dn1} & ... & ... & R_{dn(n-1)} & 0 \\ 0 & 1 & \vdots & \vdots & \vdots & 1 \end{bmatrix}^T \right)^{-1} \begin{bmatrix} 1 \\ R_{d01} \\ \vdots \\ \vdots \\ R_{d0n} \end{bmatrix}$$

$$(8)$$

finite element number for the head train shown in Fig. 6 was 181,821, with the number of nodes being 184,463. The aerodynamic load was obtained while the two trains were moving alongside each other in opposite directions (Fig. 4). As sliding meshes were used in this simulation, the trains were set as 'stationary walls' which shared the same 'adjacent cell zone' with the ground of which 'moving wall' is set.
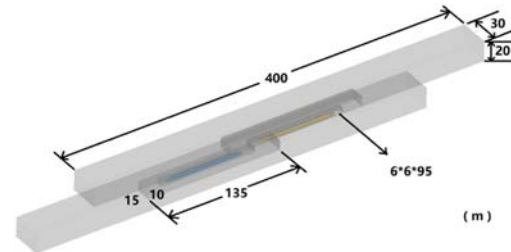

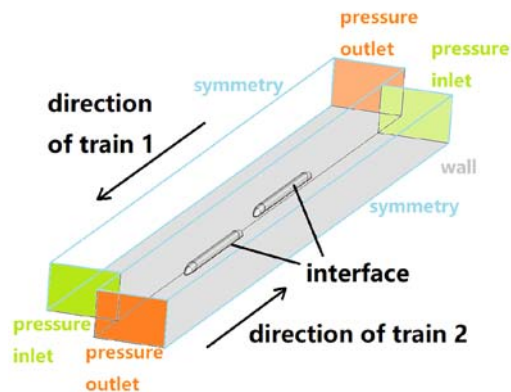**Fig. 5. Size of aerodynamical computational domain.**

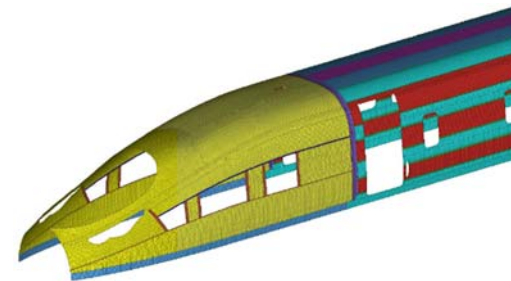**Fig. 4. Boundary conditions of two passing trains with same speed.**
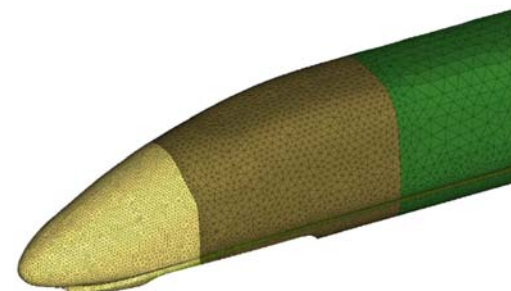

Fig. 6. Finite element mesh of head train (solid grid).
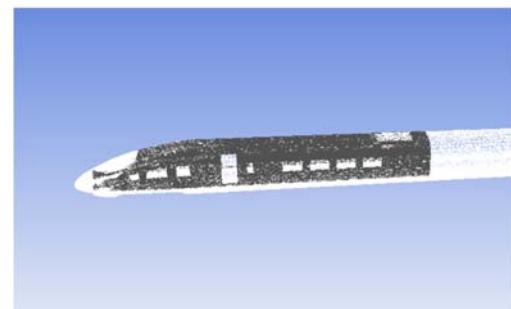

Fig. 7. Fluid surface grid of first train.

in Fig. 5. The boundary conditions are depicted in Fig. 4; the ground of the two trains is modelled as a 'moving wall' in the opposite direction at the proper speed, while the pressure inlets and outlets are all set at 0 Pascal. In addition, the total fluid computational domain is divided into two, with each train having its own subdomain, while their interface is set as the boundary condition-'interface'. Each sub-domain is also divided into three parts, as shown in Fig. 5, with the largest sub-domain, of dimensions $30 \times 20 \times 400$m, is considered the 'farfield' of this computational domain whose size has been worked out by trial calculations. The distance of two trains for the passing direction in the initial time is 20m and 1.549m is set as the distance between two trains which is perpendicular to passing direction. The fluid surface grid of the head train shown in Figure was created using an unstructured mesh while the solid side was constructed using a quadrilateral mesh, which can be seen in Fig. 6. The coupling surface of the head train is shown in the Fig. 8. Under this configuration, the number of elements for the aerodynamical computational domain was 7,383,065, the total nodes were 2,475,879, while the

Fig. 8. Coupling surface grid of first car (fluid grid is white, solid is grey).

In order to verify our passing train model, experiment results have been introduced. This

Table 1 Statistical parameters under two algorithms

Comparison parameters		Only TPS algorithm	Combined TPS with nearest interpolation algorithm
e_{P*}^r	$e_{P*,\max}^r$	3.94%	2.47%
	$e_{P*,\min}^r$	0%	0%
	$\dfrac{n(e_{P*}^r < 0.6\%)}{N}$	92.31%	93.94%
	$E(\xi_{e^r})$	0.18%	0.15%
	$D(\xi_{e^r})$	7.01275×10^{-6}	5.5×10^{-6}

experiment is designed to test the aerodynamical characteristics of 16-trainset CRH380C acrossing each other at the speed 300km/h and 350km/h in Harbin-Dalian track. We've changed our train into 16-trainset whose length is 400.5m and the results can be seen in Fig. 9. This figure shows P_{max} calculated by our simulation are closely match with experimental data whether occurring to head or tail of the train passing. The tendency of the cures is nearly the same compared to the experimental data or B-S EN 14067-4(EN BS), but the P_{min} and the value of middle plateau are not closely matched. We believe it due to the geometric model especially the aerodynamical middle train shape haven't built sophisticated. On the other hand, over fine model is really time consuming. Still, this model is enough to predict the aerodynamical characteristics of passing train.
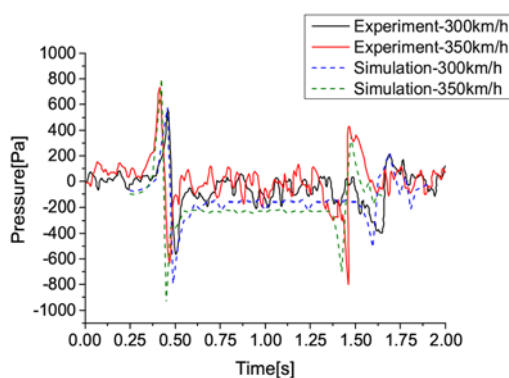

Fig. 11. Pressure values of before and after transfer on the left side of first car.

Fig. 12. Pressure values of before and after transfer on the top of first car.

Fig. 9. Experimental and simulated pressure values of 16-trainset (8M8T) high speed train CRH380C (middle train).

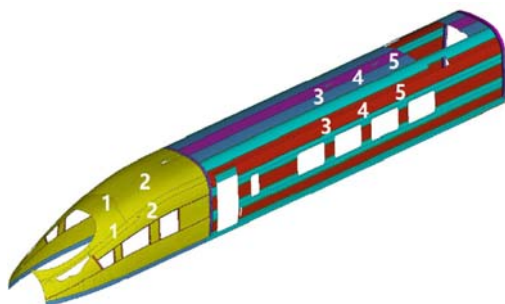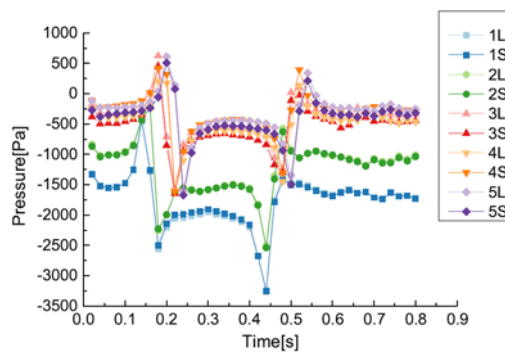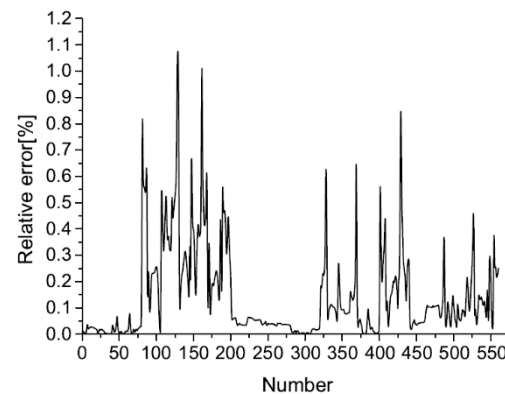**Fig. 10. Position of the picked points.**

Fig. 13. Relative errors of pressure values which Figs. 11 and 12 showed.

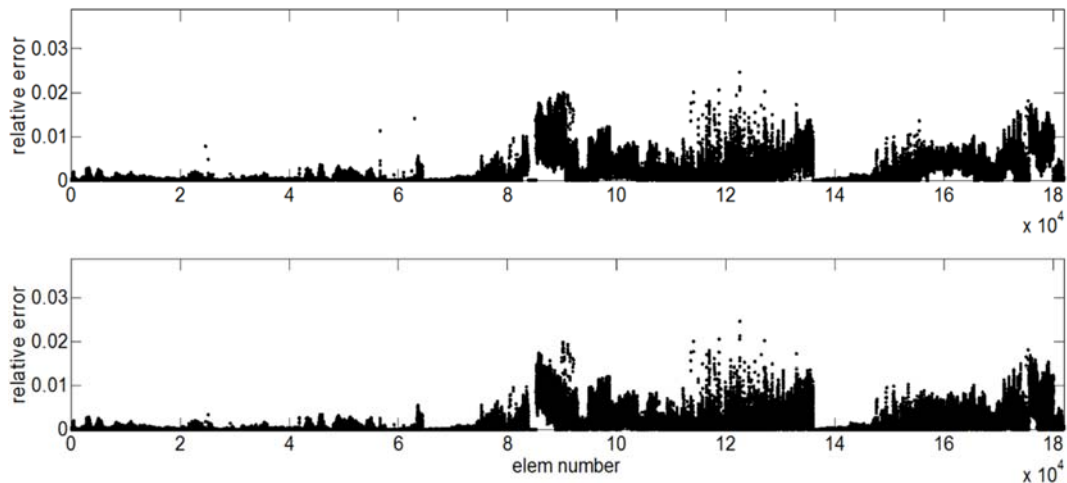The train surface pressure was calculated out via

Fig. 14. Relative errors between TPS algorithm (figure above) and TPS-Nearest interpolation algorithm (figure below).

Ansys Fluent in our 3-trainset high speed train CRH380C, then used as inputs in our own algorithms to obtain the solid surface pressure. 3-trainset has been used instead of 16-trainset is that it can reduce the computation time greatly without missing main aerodynamical characteristics of passing train. Pressure data from point 1 to 5 on the side of the first car and on the top of the car were picked out (Fig. 10). In Figs. 11 and 12, 1L represents the pressure value of the first point in the fluid domain and 1S is corresponding value in the solid domain after calculations. In addition, all the values are extracted during the time period within which the two trains' head were passing each other. The Fig. 11 shows the pressure value of 5 points on the left side and the Fig. 12 shows 5 points on the top. And it can be seen from both that the fluid and solid values were indeed coupled success-fully. In addition, considering the above values, the relative errors are shown in Fig. 13). The figure shows that the relative errors range from 0% to 1.1%, indicating that there is good agreement between the fluid domain pressure and the solid domain pressure. Figure 14 compares the relative errors between the TPS algorithm (figure above) and TPS-Nearest neighbor interpolation algorithm (figure below). The data come from the head train coupling surface when the two trainss head are crossing each other. There are 181821 pressure values in the head train. The relative errors range from 0% to 2.47% when using the TPS-Nearest interpolation algorithm and from 0% to 3.94% when using the TPS algorithm. Table 1 shows the statistical parameters under two algorithms. In particular, the relative error for two algorithms below 0.6% are 92.31% and 93.94%. In general, both methods were highly accurate.

Other statistical parameters shown in Table 1 are e^r_{P*}, i.e. the relative error of the pressure load, $\dfrac{n(e^r_{P*} < 0.6\%)}{N}$, which is the percentage rate of relative error below 0.6%, $E(\xi_{e^r})$ is the expected value of the relative error and $D(\xi_{e^r})$ is the population variance of the relative error.

5. CONCLUSIONS

We have applied a new computational approach for simulating fluid-structure interaction (FSI) problems in the complex domain of high-speed train surfaces. This approach can deal with problems such as the automatic coupling of the fluid-solid data interface, automatically identifies different mesh type, fluidic node and structural element matching and accurate data transfer. The core interpolation method combines the nearest neighbor interpolation model with the Thin Plate Spline with Tension (TPS) model. The TPS model is based on a vast scope of theoretical studies by Wu Z. M. and Frank R. *et al.* while the nearest interpolation model is from common commercial software. Our algorithms combine the high accuracy of the TPS model and the computational efficiency of the nearest neighbor interpolation model. This accuracy is validated by applying the methodology to the high-speed train FSI problem. The results show that the relative errors of 181821 pressure values in the head train are under 2.47% after using TPS-Nearest interpolation algorithm. In addition, 93.94% of the relative error values is below 0.6%. This combined approach lays the foundation for two-way FSI problems in high-speed train which are currently under development and will be presented in our future work.

REFERENCES

Appa, K. (1989). Finite-surface spline. Journal of Aircraft 26(5), 495–496.

Bell, J., D. Burton, M. Thompson, A. Herbst, and J. Sheridan (2014). Wind tunnel analysis of the slipstream and wake of a high-speed train. Journal of Wind Engineering and Industrial Aerodynamics 134, 122–138.

Benbourhim, M. and A. Bouhamidi (2005). Approximation of vectors fields by thin plate s-plines with tension. Journal of Approximation Theory 136, 198–229.

Boer, A., A. Zuijlen and H. Bijl (2007). Re- view of coupling methods for non-matching meshes. Computer Methods in Applied M-chanics and Engineering 196(8), 1515–1525.

EN BS. 14067-4: 2005+ a1: 2009. BSI railway applicationsaerodynamics Part 4.

Farhat, C., M. Lesionne and P. LeTallec (1998). Load and motion transfer algorithms for fluid/structure interaction problems with non-matching discrete interfaces: Momentum and energy conservation, optimal discretization and application to aeroelasticity. Computer Methods in Applied Mechanics and Engineering 157, 95–114.

Frank, R. (1982). Scattered data interpolation: tests of some methods. Mathematics Computation 38, 191–200.

Goura, G., K. Badcock, M. Woodgate and B. Richards (2001). A data exchange method for fluid-structure interaction problems. The Aeronautical Journal 105(1046), 215–221.

Harder, R. L. and R. N. Desmarais (1972). Interpolation using surface splines. Journal of aircraft 9(2), 189–191.

Hermann, G., Matthies, N. Rainer and S. Jan (2006). Algorithms for strong coupling procedures. Computer methods in applied mechanics and engineering 195, 2028–2049.

Keith, S., B. Richard, K. Vinay and E. T. Tayfun (2000). Parachute fluid-structure interactions:3-d computation. Comput. Methods Appl. Mech. Engrg 190, 373–386.

Lohner, R., C. Yang and J. Cebral (1998). Fluid-structure interaction using a loose coupling algorithm and adaptive unstructured grids. p-p. 1–16. America: AIAA Paper.

Pidaparti, R. (1992). Structural and aerodynamic data transformation using inverse isoparametric mapping. Journal of Aircraft 29, 507–509.

Shepard, D. (1968). A two-dimensional interpolation function for irregularly-spaced data. In Proceedings of the 1968 23rd ACM national conference, pp. 517–524. ACM.

Smith, J. M., E. C. Cesnik and H. D. Hodges (1995). An evaluation of computational algorithms to interface between cfd and csd methodologies. GEORGIA INST OF TECH ATLANTA SCHOOL OF AEROSPACE ENGINEERING.

Smith, M. and D. Hodges (2000). Evaluation of some data transfer algorithms for noncontiguous meshes. Aerospace. Engrg. 13(2), 52–58.

Smith, M. J., D. H. Hodges and C. Cesnik (1995). An evaluation of computational algorithms to interface between cfd and csd methodologies. Wright-Patterson Air Force Base Report No. WL-TR-96-3055, 1–45.

Su, B., R. Qian and X. Yuan (2010). Advances in research on theory and method of data exchange on coupling interface for fsi analysis [j]. Spatial Structures 1, 002.

Tayfun, E. T., S. Sunil, K. Ryan and S. Keith (2006). Space-time finite element techniques for computation of fluid-structure interactions. Comput. Methods Appl. Mech. Engrg. 195, 2002–2027.

Thévenaz, P., T. Blu and M. Unser (2000). Interpolation revisited [medical images application]. IEEE Transactions on medical imaging 19(7), 739–758.

Tiago, C. and V. Leitão (2006). Application of radial basis functions to linear and nonlinear. Computers and Mathematics with Applications 151(8), 1311–1334.

Wu, Z. (1995). Multivariate compactly supported positive definite radial functions. Advances in Computational Mathematics 4, 283–292.

Xu, S. and M. Chen (2004). Study of date exchange metod for coupling computational cfd/csd. Chinese Journal of Applied Mechanics 2, 005.

Zhang, W. (2013). Dynamics of coupling systems in high-speed train theory and practice (China). Beijing, China: Beijing Science Press.